

# Using Finite Element Method in geotechnical design. Soil constitutive laws and calibration of the parameters. Retaining wall case study

HORATIU POPA, LORETTA BATALI  
 Geotechnics and Foundations Department  
 Technical University of Civil Engineering of Bucharest  
 124 Bd. Lacul Tei, Bucharest  
 ROMANIA  
 horatiu@utcb.ro    loretta@utcb.ro    www.utcb.ro

*Abstract:* - Using FEM for geotechnical design of constructions with high impact of the soil – structure interaction is a common practice. However, for obtaining results close to the real behavior of the analyzed structures it is required to use complex constitutive models for all materials, especially for describing the soil behavior. Paper presents the differences in the numerical modeling when three different constitutive laws are used: one linear elastic – perfectly plastic and two nonlinear elastic - hardening plastic laws. Comparisons between numerical modeling and laboratory tests are presented in order to emphasize the differences between the constitutive laws and to calibrate their parameters. As well, a numerical calculation using FEM for an embedded retaining wall is presented, using different soil constitutive models. The results regarding the displacements of the wall and the bending moments in the wall are compared with the experimental values.

*Key-Words:* - numerical modeling, finite element method, soil mechanics, Mohr-Coulomb, Nova, Vermeer, retaining wall

## 1 Introduction

The materials used in civil engineering have been and still are continuously studied in order to obtain effective design of the structures. For the design calculations materials (concrete, steel, soil etc.) are assimilated with continuous media. As every continuous medium, these are governed by physical and mechanical principles (as, for example, the energy conservation principle). However, the general physical laws don't allow making the difference between various material behaviors.

Thus, it is desired to characterize the specific behavior of the continuum and its equivalence with the studied material. This is the constitutive law associated with the specific material and it has to describe the material evolution under external actions. Knowing this constitutive law is indispensable for having a complete equations system for any continuum medium mechanics or structural calculation problem. Diversity and complexity of materials led to emphasize a complex behavior too: elasticity, viscosity, plasticity and combinations of those.

Soils represent, by their composition itself, a complex, heterogeneous material, having a strongly non-linear response under load, [1]. For this reason the constitutive laws associated to various soil types (cohesive, non-cohesive, saturated or unsaturated etc.), [2], are continuously developed and improved.

In this framework, FEM applications for geotechnical design of structures for which soil – structure interaction

is important, [3], [4], (e.g. retaining structures, dams, bridges, special foundations etc.) allow using more and more complex constitutive laws for describing the material behavior. However, more complex the law, more difficult to estimate the defining parameters.

The following paragraphs are describing some of the typical soil constitutive laws. First of all is presented the Mohr – Coulomb criterion, a linear elastic – perfect plastic model, which is probably the most used for modeling soils. The large use of this model is due to its simplicity and to the easiness of determining the specific parameters.

Two other constitutive laws, more evolved, nonlinear elastic – hardening plastic are also presented, meaning Nova and Vermeer. The specific equations are presented and their ability for modeling soils is judged through comparisons with experimental results.

A practical case study is also used for comparison: a retaining wall used for supporting a deep excavation.

## 2 Constitutive laws for soils

Soils are a heterogeneous material whose behavior is strongly influenced by various factors as: grain size, mineralogy, structure, pore water, initial stress state etc. Moreover, soils are characterized by time dependent modifications (creep), thus having a strong rheological character.

For this reason the constitutive laws associated to soils are numerous and various, using one or other being dependent of soil type, of problem to be solved and, most of the time, of the possibilities of estimating complex parameters.

**2.1 Mohr-Coulomb model**

Coulomb proposed the first plasticity model in soil mechanics. It is composed of two symmetrical lines in Mohr’s plane ( $\sigma, \tau$ ), having an angle  $\phi$  with the normal stresses axis,  $\sigma$  and having as equation, [5]:

$$F(\sigma_{ij}) = \sigma_1 - \sigma_3 - (\sigma_1 + \sigma_3) \sin \phi - 2c \cos \phi \leq 0 \quad (1)$$

where  $\sigma_1$  and  $\sigma_3$  are the extreme main stresses.

Parameter  $c$  represents the soil cohesion, while  $\phi$  is the internal friction angle. In the space of main stresses ( $\sigma_1, \sigma_2, \sigma_3$ ) the surface defined by function  $F$  is a pyramid with hexagonal section having as axis the line  $\sigma_1 = \sigma_2 = \sigma_3$  (figure 1).

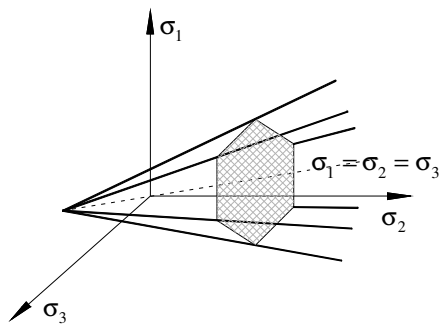


Fig. 1. Representation of Mohr-Coulomb criterion in main stresses space

The plastic potential defined as a function of the extreme main stresses is:

$$G(\sigma_{ij}) = \sigma_1 - \sigma_3 + (\sigma_1 + \sigma_3) \sin \psi + \text{const} \quad (2)$$

where  $\psi$  is the dilatancy angle ( $\psi = \phi$  if it is an associated criterion).

The elasticity associated to the Mohr – Coulomb criterion is a linear isotropic – Hooke type one. The criterion contains 5 mechanical parameters:

- $E$  – elasticity modulus,  $\nu$  - Poisson’s coefficient: elastic parameters;
- $c, \phi, \psi$ : plastic parameters.

**Determination of Mohr – Coulomb criterion parameters**

The parameters of the Mohr – Coulomb criterion can be determined using a triaxial compression, axial symmetric laboratory test. Figure 2 presents the results of such a test and the manner in which the parameters can be determined ( $\epsilon_1$  – main specific strain;  $\epsilon_v$  – volumetric strain).

If the soil cohesion is not nil (cohesive soils), a minimum of two laboratory tests are required, conducted under different consolidation pressures, for determining the parameters  $\phi$  and  $c$ . For each test, the axial stress at failure,  $\sigma_1$  and the consolidation pressure are plotted in the  $((\sigma_1 + \sigma_3)/2, (\sigma_1 - \sigma_3)/2)$  axis system. The obtained points are approximated by a linear regression. The slope of the line ( $\sin \phi$ ) provides the  $\phi$  value, while the ordinate for  $x = 0$  ( $c \cos \phi$ ) gives the  $c$  value (figure 3).

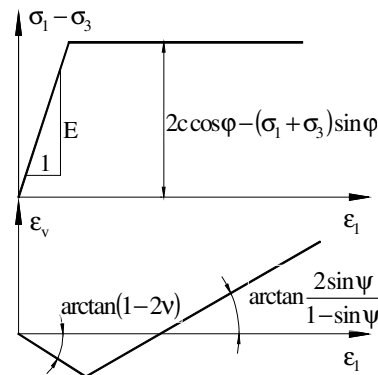


Fig. 2. Axial symmetric triaxial compression test modeled using Mohr – Coulomb criterion

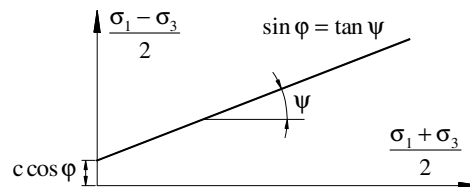


Fig. 3. Determination of parameters  $\phi$  and  $c$

**2.2 Nova model**

Nova model, [6], is a nonlinear elastic – hardening plastic criterion, with isotropic plastic hardening, inspired by the Cam-clay model, [5], but adapted to sand behavior.

It has been developed based on tests conducted on cylindrical sand samples, which explains the formulation as a function of stress invariants,  $p$  (mean pressure) and  $q$  (deviatoric stress) and plastic strain invariants,  $\epsilon_v^p$  (plastic volumetric strain) and  $\epsilon_d^p$  (plastic deviatoric strain).

The elastic component of the strain is linked to the stress state by the following incremental relationship:

$$d\epsilon_{ij}^e = L_o d\eta_{ij} + B_o \frac{dp}{3p} \delta_{ij} \quad (3)$$

where  $L_o$  and  $B_o$  are two specific parameters of the

model and  $\eta_{ij} = \frac{\sigma_{ij} - p\delta_{ij}}{p}$ , ( $\delta_{ij}$  is Kroneker's tensor).

The mean pressure,  $p$  and the deviatoric stress,  $q$  are calculated using the following formulas:

$$p = \frac{\sigma_1 + \sigma_2 + \sigma_3}{3} \quad q = \sqrt{\frac{(\sigma_1 - \sigma_2)^2 + (\sigma_1 - \sigma_3)^2 + (\sigma_2 - \sigma_3)^2}{2}} \quad (4)$$

The expressions for the yield surface and plastic potential are given in table 1.

Table 1. Yield surface and plastic potential expressions function of stress state

Stress state	Stress – dilatancy relationship	Yield surface $F(p, q, p_c)$ and plastic potential $G(p, q, p_c)$
$\frac{q}{p} \leq \frac{M}{2}$	$\frac{d\varepsilon_v^p}{d\varepsilon_d^p} = \frac{M^2 p}{4\mu q}$	$F(p, q, p_c) = G(p, q, p_c)$ $G(p, q, p_c) = \frac{4\mu}{M^2} - \frac{q^2}{p^2} + 1 - \frac{p_c^2}{p^2}$
$\frac{q}{p} \geq \frac{M}{2}$	$\frac{d\varepsilon_v^p}{d\varepsilon_d^p} = \frac{M}{\mu} - \frac{q}{\mu p}$	$F(p, q, p_c) = \frac{q}{p} - \frac{M}{2} + \min\left(\sqrt{1 + \mu} \frac{p}{p_c}\right) = 0$ $G(p, q, p_c) = \frac{q}{p} - \frac{M}{1 - \mu} \left[1 - \mu \left(\frac{p}{p_{sp}}\right)^{\frac{1 - \mu}{\mu}}\right] = 0$

Figure 4 presents the yield surface and the plastic potential for Nova's criterion in  $(p, q)$  plane.

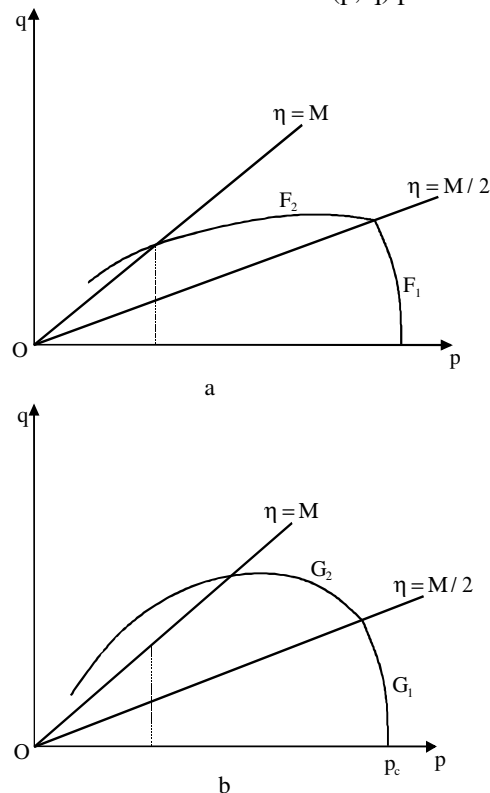


Fig. 4. Yield surface (a) and plastic potential (b) for Nova's criterion

Variables  $p_{co}$  and  $p_c$  correspond to the intersection of the plastic potential with the isotropic compression axis for  $\frac{q}{p} \geq \frac{M}{2}$  and to the variable characterizing the

hardening, respectively.  $p_c$  is function of the plastic strain invariants:

$$p_c = p_{co} \exp\left(\frac{\varepsilon_v^p + D\varepsilon_d^p}{1 - B_o}\right) \quad (5)$$

where:

$$\varepsilon_v^p = \varepsilon_1^p + \varepsilon_2^p + \varepsilon_3^p \text{ and}$$

$$\varepsilon_d^p = \sqrt{\frac{(\varepsilon_1^p - \varepsilon_2^p)^2 + (\varepsilon_1^p - \varepsilon_3^p)^2 + (\varepsilon_2^p - \varepsilon_3^p)^2}{2}} \quad (6)$$

### Determination of Nova's criterion parameters

Nova's criterion is described by eight parameters determined based on triaxial - axial symmetric compression tests, in drained conditions, with one unloading - reloading cycle, [7].

- **B<sub>o</sub>**: elastic behavior parameter determined by the points on the unloading curve. These points form a line in the  $(\varepsilon_v^e, \ln p)$  plan; the slope of this line provides  $B_o$  value.
- **L<sub>o</sub>**: elastic behavior parameter determined by the points on the unloading curve. These points form a line in  $(\varepsilon_d^e, q/p)$  plan, which slope gives  $L_o$  value.
- **I**: parameter linked to the initial tangent to the behavior curve  $(\varepsilon_1, q)$ :  $\frac{dq}{d\varepsilon_1} (\sigma_1 = \sigma_3) = \frac{9\sigma_3}{6L_o + 1}$ .
- **D**: parameter modeling the dilatancy.  $D$  is the limit of  $d\varepsilon_v^p / d\varepsilon_d^p$  when the failure is approaching.
- **M**: parameter related to the extreme point of the plastic volumetric strain ( $d\varepsilon_v^p = 0$ ).  $M$  can be determined from the  $(\varepsilon_1, \varepsilon_v^p)$  graph. The strain  $\varepsilon_v^p$  is evaluated as the difference between the experimental volumetric strain (or total strain) and the elastic volumetric strain calculated using Nova's criterion ( $B_o$  being known).
- **μ**: parameter related to the soil sample failure. It is determined using the relationship:  $\mu = (\eta_f - M) / D$ , where  $\eta_f$  corresponds to stress rate  $q / p$  at failure.
- **m**: parameter related to the position of the characteristic state (the extreme point of the volumetric strain,  $d\varepsilon_v = 0$ ). Its determination is delicate and often is preferred to be adjusted successively based on an estimated value of the characteristic state. The equation of the tangent to the curve  $(\varepsilon_1, q)$  for the point  $(\varepsilon_1, d\varepsilon_v = 0)$  can be written and the following relationship is deduced:

$m = \frac{-(1 - B_o)(3 - \eta_c)(M - \eta_c)}{\mu B_o D + l(M - \eta_c)}$ , where  $\eta_c$  is the stress rate  $q/p$  for the characteristic state.

▪  $p_{co}$ : parameter depending on the initial state, equal to the consolidation pressure of a triaxial test or calculated function of initial stress state so that no initial elastic domain exists into the soil mass.

As the parameters of the Nova's criterion haven't an obvious physical signification as the Mohr – Coulomb parameters it is difficult to quantify their influence on the soil behavior.

**2.3 Vermeer's model**

The constitutive model developed by Vermeer, [8], is a nonlinear elastic – hardening plastic model also, with two hardening mechanisms. The first hardening mechanism is a pure volumetric one (consolidation), while the second one is purely deviatoric (shear). The plastic potential coincides with the yield surface for the first mechanism (associated potential), while for the second mechanism a relationship type stress – dilatancy is used for the plastic potential. The elastic part of the criterion is non-linear and isotropic and derives from a potential.

The elastic component of the Vermeer's model is based on Hooke elasticity with a Young's modulus depending on the stress state and a nil Poisson's coefficient. The relationship linking stresses and strains is the following:

$$\sigma_{ij} = 2\varepsilon_{ij}G_s(\sigma_{ij}) \quad \text{with} \quad G_s(\sigma_{ij}) = G_o[\sigma_n/p_o]^{(1-\beta)} \quad (7)$$

where  $p_o$  is an initial isotropic reference pressure for which the volumetric strain is  $\varepsilon_o^c$  ( $2G_o\varepsilon_o^c = 3p_o$ ),  $\beta$  is a constant and  $\sigma_n$  represents the following stress invariant:

$$\sigma_n^2 = \frac{\sigma_1^2 + \sigma_2^2 + \sigma_3^2}{3} \quad (8)$$

The volumetric yield surface has the following expression:

$$F_v(\sigma_{ij}, \varepsilon_{ij}^p) = G_v(\sigma_{ij}, \varepsilon_{ij}^p) = \varepsilon_o^c[\sigma_n/p_o]^\beta - \varepsilon_{vc}^p = 0 \quad (9)$$

where  $\varepsilon_o^c$  is a constant and  $\varepsilon_{vc}^p$  represents the hardening parameter of the yield surface.

The deviatoric yield surface has the following expression:

$$F_c(\sigma_{ij}, \varepsilon_{ij}^p) = -3p\Pi_2 + \text{III}_3A(x) = 0 \quad (10)$$

where  $p$ ,  $\Pi_2$ ,  $\text{III}_3$  are the classical invariants using the sign convention of the continuum medium mechanics:

$$p = -(\sigma_1 + \sigma_2 + \sigma_3)/3; \quad \Pi_2 = -\sigma_1\sigma_2 - \sigma_1\sigma_3 - \sigma_2\sigma_3; \quad \text{III}_3 = -\sigma_1\sigma_2\sigma_3 \quad (11)$$

$A(x)$  is a scalar function defined as follows:

$$A(x) = \frac{27(3+h(x))}{(2h(x)+3)(3-h(x))} \quad c = \frac{6\sin\phi_p}{3 - \sin\phi_p} \quad (12)$$

$$h(x) = \sqrt{x^2/4 + cx} - x/2 \quad x = \gamma^p 2G_o[p_o/\sigma_n]^\beta/p_o$$

where  $c$  is a parameter defined function of the maximum internal friction angle  $\phi_p$  and  $\gamma^p$  represents the plastic distortion:  $\gamma^p = (e_{ij}^p e_{ij}^p / 2)^{0.5}$ .

These complex expressions cover a very simple reality. In fact, the deviatoric yield surface was built so that it is reduced to Drucker-Prager's criterion [5] when the conditions of a triaxial axial symmetric test conditions are fulfilled. In this case, the yield surface equation is reduced to the following simple relationship:

$$F_c = q/p - h(x) = 0 \quad (13)$$

The plastic potential is not associated and it is built using the following relationship:

$$G_c(\sigma_{ij}) = \sqrt{2s_{ij}s_{ij}/3 - 4p(\sin\psi_m)/3} \quad (14)$$

By definition, angle  $\psi_m$  is the dilatancy angle which is related to the stress state by the following expression:

$$\sin\psi_m = \frac{\sin\phi_m - \sin\phi_{cv}}{1 - \sin\phi_m \sin\phi_{cv}} \quad (15)$$

where  $\phi_{cv}$  is the internal friction angle at constant volume. Angle  $\phi_m$  is related to the stress state by:

$$\sin\phi_m = \frac{\sqrt{9 - A(x)}}{1 - A(x)} = \frac{3q}{6p + q} \quad (16)$$

Failure for Vermeer model is obtained for the following stress rate  $(q/p)_r$ :

$$(q/p)_r = \frac{6\sin\phi_p}{3 - \sin\phi_p} \quad (17)$$

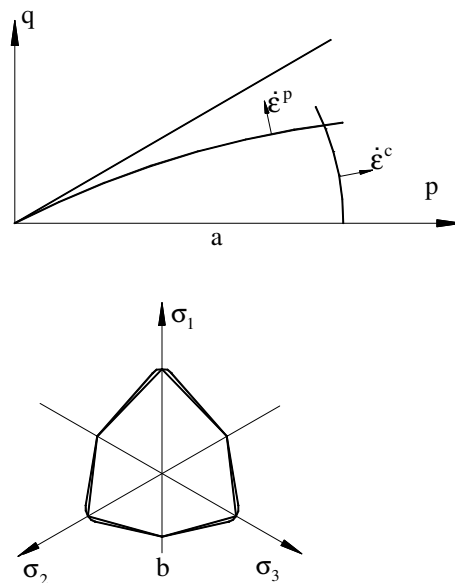


Fig. 5. Volumetric yield surface (a) and deviatoric yield surface (b) for Vermeer's model

Thus, Vermeer model has six parameters:  $\phi_p$ ,  $\phi_{cv}$ ,  $\epsilon_o^c$ ,  $\epsilon_n^c$ ,  $\beta$  and  $p_o$ . The reduced number of parameters represents an important advantage in using this constitutive law. Figure 5 presents the volumetric and the deviatoric yield surfaces for Vermeer’s model.

**Determination of Vermeer’s model parameters**

As for Nova’s criterion, the parameters of Vermeer’s model are determined based on triaxial compression - axial symmetric tests, in drained conditions and with one unloading – reloading cycle, [9].

▪  $\epsilon_o^c$  and  $\beta$ : elastic behavior parameters determined for the unloading curve. These points form a line on the  $(\ln \epsilon_n^c, \ln \sigma_n)$  graph. The equation of this line is:  $\ln \epsilon_n^c = \beta \ln(p_o / \sigma_n) + \ln(\epsilon_o^c / 3)$ , with  $\epsilon_n^c = (\epsilon_{ij}^c \epsilon_{ij}^c / 3)^{0.5}$  and  $\sigma_n = (\sigma_{ij} \sigma_{ij} / 3)^{0.5}$ .

▪  $\epsilon_o^c$ : parameter related to the initial tangent to the graph  $(\epsilon_1, q)$ ,  $\frac{dq}{d\epsilon_1}(\sigma_1 = \sigma_3) = \frac{9\sigma_3}{\epsilon_o^c(2 + \beta) + \epsilon_o^c\beta}$ .

▪  $\phi_p$ : parameter related to the soil sample failure;  $\phi_p$  is the maximum friction angle.

▪  $\phi_{cv}$ : parameter related to dilatancy modeling. Angle  $\phi_{cv}$  is determined using the following relationship:

$$\sin \phi_{cv} = \frac{\sin \phi_p - \sin \psi_m}{1 - \sin \phi_p \sin \psi_m} \text{ with } \sin \psi = \frac{3d\epsilon_v}{4(d\epsilon_3 - d\epsilon_1)},$$

where  $\psi$  represents the dilatancy angle during the test and  $\psi_m$  is its limit before failure.

▪  $p_o$ : parameter depending on the initial state, equal to the consolidation pressure for a triaxial compression test or calculated function of the initial state so that no initial elastic domain exists in the soil mass.

**3 Calibration of constitutive law parameters based on numerical FEM modeling**

As it has been seen previously, the difficulty in obtaining the parameters of constitutive laws is direct proportional with laws complexity. In general, they suppose triaxial tests with imposed stress path, which is not easily done by ordinary geotechnical laboratories.

Even after a proper determination of the parameters, before their use in numerical calculation for structural design is necessary to calibrate them. This is done through numerical modeling of the same experimental tests giving the laws parameters, [10]. The following paragraphs present such numerical calculations for the three constitutive models described above. The soil is a fine, poorly graded, dry sand.

**3.1 Calibration of Mohr-Coulomb criterion parameters**

The results obtained by FEM modeling of the triaxial test providing the parameters of this model are shown figure 6. The consolidation pressure of the sand sample was 60 kPa.

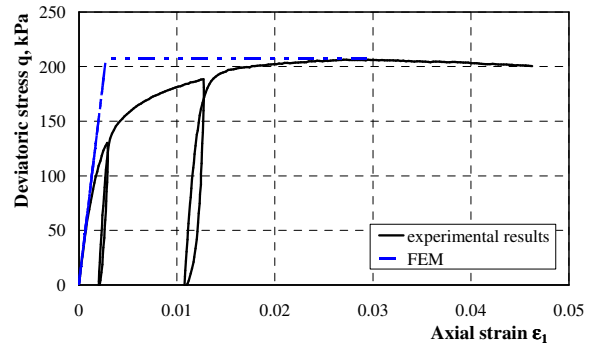


Fig. 6. Calibration of the Mohr-Coulomb parameters

On the graph figure 6 one can note a good approximation of the initial elastic modulus, as well as of the failure stresses. Being an elastic – perfectly plastic criterion, Mohr – Coulomb model cannot model the yield and, as a consequence, the curvature of the experimental results (graph  $q - \epsilon_1$ ) cannot be seen.

**3.2 Calibration of Nova’s criterion parameters**

Based on the triaxial tests conducted under a consolidation pressure of 60 kPa, 4 FEM analyses have been performed. The Nova parameters used for these models are presented table 2, while the graphs – curves  $(\epsilon_1, q)$  and  $(\epsilon_1, \epsilon_v)$  - are shown figures 7 and 8, respectively.

Table 2. Nova’s model parameters – FEM analyses of the triaxial test

FEM	$B_o$	$L_o$	$m$	$l$
1	0.000185	0.000597	0.167	0.00107
2	0.0002	0.00061	0.793	0.00113
3	0.00022	0.00065	0.8	0.0013
4	0.0002	0.00065	0.719	0.0031
FEM	D	M	$\mu$	$p_{co}$ kPa
1	0.587	1.294	0.62	60
2	0.582	1.224	0.647	60
3	0.58	1.26	0.64	60
4	0.586	1.279	0.62	60

As it can be seen on the graphs figures 7 and 8, the differences between the experimental curves and the theoretical ones are quite important. Even if the failure stresses are properly modeled numerically, the plastic strains and the slope of the  $(\epsilon_1 - q)$  graph are not well approximated. By analyses no. 1 and 4 it was tried to

obtain a more ample plastic response, but the elastic strains are not well modeled and the position of the characteristic state is very different than the experimental one (graph  $\epsilon_1, \epsilon_v$ ). However, in the analyses no. 2 and 3 the position of the characteristic state is closer than the real one and the initial slope of the curve  $\epsilon_1 - q$  is the same as the experimental one. The plastic response is, however, more reduced than the real one.

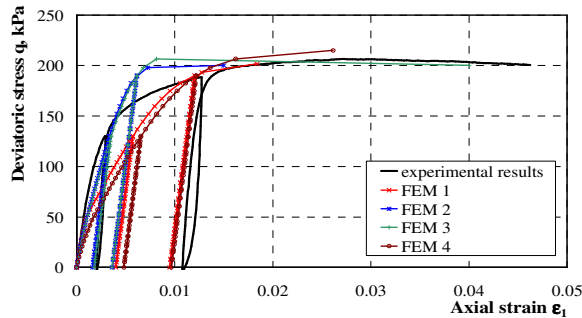


Fig. 7. Calibration of the Nova's model parameters, graph  $\epsilon_1 - q$

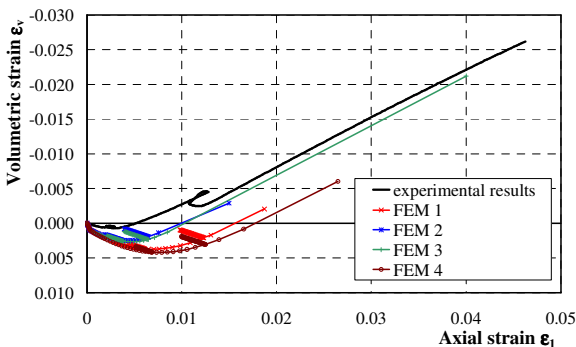


Fig. 8. Calibration of Nova's model parameters, graph  $\epsilon_1 - \epsilon_v$

### 3.3 Calibration of Vermeer's model parameters

For the triaxial test under a consolidation pressure of 60 kPa, 5 finite element analyses have been used for calibrating the parameters of the Vermeer's criterion. The values used for the analyses are presented table 3, while the graphs in figures 9 and 10.

Table 3. Vermeer's model parameters – FEM analyses of the triaxial test

FEM	$\epsilon_o^c$	$\phi_{cv}$	$\phi_p$	$\beta$	$\epsilon_o^c$	$P_{co}$ kPa
1	0.003	26.2	42.1	0.87	0.004	60
2	0.0037	30	42.1	0.72	0.0048	60
3	0.002	25	40.5	0.38	0.0028	60
4	0.002	24	40.7	0.32	0.0025	60
5	0.0018	23	40.3	0.29	0.0022	60

As it can be observed on the graphs figures 9 and 10, the parameters of the first two FEM analyses are poorly approximating the sand sample response. But the three following FEM analyses are close to the real response, being able to estimate quite accurately the two graphs -  $\epsilon_1 - q$  and  $\epsilon_1 - \epsilon_v$ . Opposite to Nova's criterion, a better estimation of both elastic and plastic part is observed and the position of the unloading – reloading cycles is, also, accurate compared to the experiment.

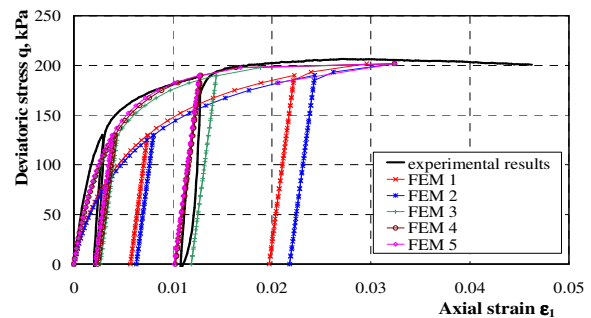


Fig. 9. Calibration of Vermeer's model parameters, graph  $\epsilon_1 - q$

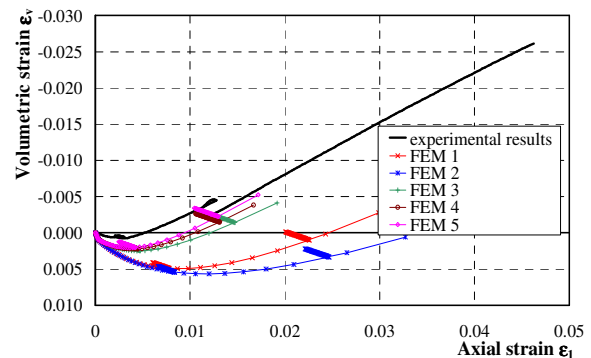


Fig. 10. Calibration of Vermeer's criterion, graph  $\epsilon_1 - \epsilon_v$

## 4 Case study. Retaining wall

Retaining walls are often used for supporting deep excavations, especially in urban areas. The correct estimation of their behavior is very important taking into account the impact on the neighboring buildings. The influence of a retaining structure can extend up to 2 – 3 times the excavation depth. The parameters influencing the wall behavior are numerous and difficult to consider and the classical methods based on limit equilibrium do not offer the possibility of estimating them [11]. FEM is offering the best of modeling possibilities if an adequate numerical model, with correct and calibrated values is used.

The FEM numerical modeling parameters influencing decisively the calculation results are [12]:

- two and three-dimensional analysis;
- model size;

- mesh generation;
- constitutive laws used for the soil and retaining wall;
- initial stress state acting into the ground;
- retaining wall construction;
- excavation and retaining structure loading.

Here below is presented the numerical modeling using FEM of an embedded retaining wall. The numerical analysis was carried out using the CESAR-LCPC finite element code.

#### 4.1 Geometrical characteristics of the retaining wall

The modeled retaining wall represents an experimental laboratory model (Laboratoire Central des Ponts et Chaussées – LCPC, Nantes) which has been studied in the centrifuge [13], [14].

Figure 11 shows the overall size of the model, which corresponds to the real prototype modeled by laboratory tests. The lateral and lower limits imposed by the container in which the experimental model has been created are also the limits of the numerical model.

Figure 11 presents also the boundary conditions used in the numerical modeling (no lateral displacements for the vertical boundaries and nil vertical displacement along the lower boundary).

The total height of the retaining wall is 10 m, while the excavation can reach a maximum depth of 6 m.

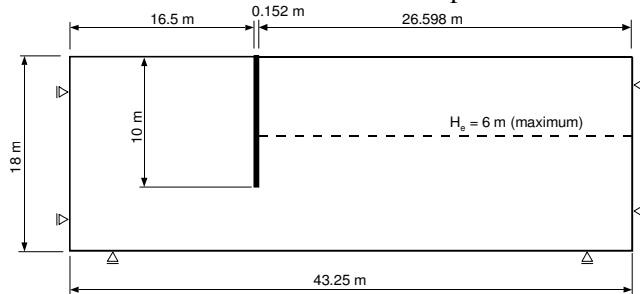


Fig. 11. Geometrical characteristics

#### 4.2 Numerical model characteristics

##### 4.2.1 Finite element mesh

Figure 12 shows the finite element mesh, while in table 4 the characteristics of the finite elements are indicated. The computations were performed in 2D, taking into account the fact that the experimental procedure imposed a two-dimensional behavior of the wall. The numerical computations refer to the prototype modeling, corresponding to the small-scale model tested in the centrifuge.

The wall and the soil are modeled by 8-noded plane strain elements. This mesh density agrees to a reasonable computing time and a good accuracy of the results. In

order to reproduce the interaction between the wall and the soil, a layer of special elements is incorporated at the interface area (contact elements - quadrilateral 6-noded elements).

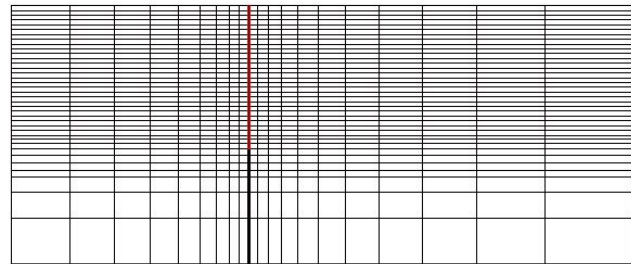


Fig. 12. Finite element mesh

Table 4. Mesh characteristics

Number of nodes	Number of elements
2686	876

##### 4.2.2 Material characteristics

The soil used for the experimental model is a dry fine sand with a dry unit weight  $\gamma_d = 16.0 \text{ kN/m}^3$ .

In order to model the soil behavior, two constitutive laws were used: Mohr – Coulomb criterion and Vermeer criterion. The values of the parameters as they have been used in calculations are shown table 5.

Table 5. Values of the soil constitutive laws parameters

Mohr-Coulomb						
E, MPa	$\nu$	c, kPa	$\phi, ^\circ$	$\psi, ^\circ$		
75 or 10	0.275	0	39.4	16.7		
Vermeer						
E, MPa	$\epsilon_o^c$	$\phi_{cv}$	$\phi_p$	$\beta$	$\epsilon_o^c$	$p_{co}$ , kPa
75	0.0018	23	40.3	0.29	0.0022	60

As it can be seen in table 5, in case of Mohr – Coulomb criterion two values of the elasticity modulus have been used: 75 MPa, which is the real modulus of the soil and another value, much lower, of 10 MPa, used for improving the numerical results and make them closer to the experimental values.

For Vermeer's criterion the parameters were obtained by calibration with laboratory tests (see paragraph 3.3).

The contact between soil and wall has been modeled using a sliding interface with same parameters for all calculations. This interface type has been chosen after many numerical calculations using various interface types and the results indicated the sliding interface to be the one modeling the best the interaction for the studied case, [10]. The sliding interface is characterized by an elasticity modulus equal to the soil one and it has zero traction strength.

For the wall an elastic constitutive law was adopted, taking into account that it is much stiffer than the soil.

The wall is a metallic one (sheet-pile type) having an elasticity modulus  $E_w = 22350 \text{ MPa}$  and a Poisson's coefficient  $\nu_w = 0.3$ .

**4.2.3 Calculation stages**

Generally, the numerical calculations followed the stages presented here below:

- stage 0 – calculation of the initial stress state within the soil. This stage is indispensable for an excavation work, in order to calculate and apply the excavation forces on the pit surfaces. The initial stresses have to be calculated and not issued from a simple initialization; without this, the stresses in the contact elements are nil. For this stage a special loading module of the software has been used, allowing the stress calculation function of the dead load of the material. When passing to the following numerical stage, the deformations calculated in the first stage have to be cancelled.
- stages 1...6 – modeling of the excavation by 1.0 m thick layers until attempting the non – convergence of the calculation process or the maximum value imposed at 6.0 m depth.

All the calculation stages were decomposed into 10 load increments in order to take into account the soil non-linearity.

Due to large time required for reaching the convergence for high excavation depths, especially in case of Vermeer's criterion, the numerical calculations were stopped for a maximum excavation depth of 4.0 m.

**4.2.3 Results of numerical modeling and comparison with the experimental data**

The calculation results for the maximum horizontal displacements of the retaining wall are shown fig. 13.

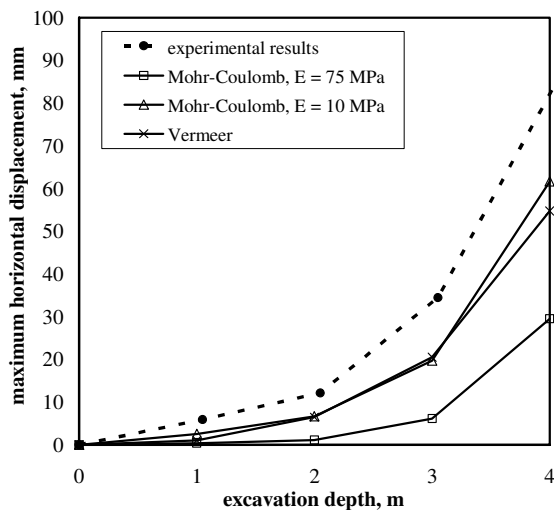


Fig. 13. Maximum horizontal displacements of the retaining wall

As one can note on the graph figure 13, Mohr – Coulomb criterion for the real elasticity modulus  $E = 75 \text{ MPa}$  is not approximating adequately the retaining structure behavior. Differences between numerical and experimental results are very large (over 200 %). An improvement can be obtained using a severe diminution of the elasticity modulus to 10 MPa, thus the differences being reduced to 30 – 70 %. Even in this case Mohr – Coulomb criterion underestimates the lateral displacements of the wall.

By using Vermeer's criterion an underestimation of the displacements was also obtained, but for the real characteristics of the soil, an adjustment of the parameters not being required. In fact, the results obtained with Mohr – Coulomb model for 10 kPa elasticity modulus are superposing quite well to the results obtained using Vermeer's criterion.

Figure 14 shows a comparison between calculations and experimental results for wall displacements.

One can note that the deformation shape is well approximated, but the values are underestimated.

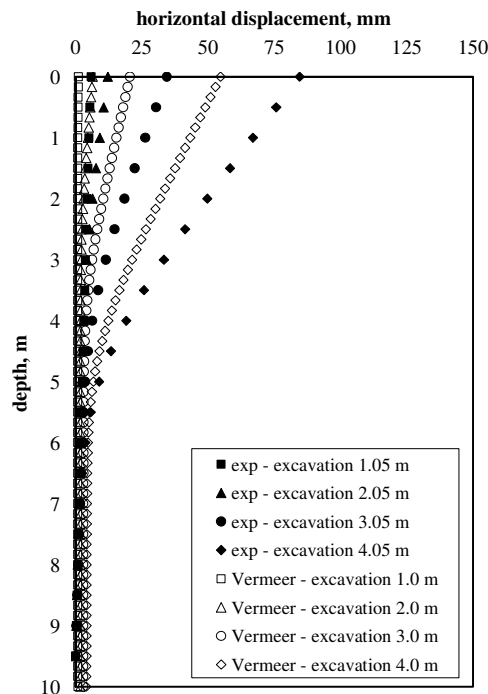


Fig. 14. Horizontal displacements of the retaining wall

As far as the wall maximum bending moments are concerned, their evolution is presented figure 15.

In this case it can be noted that Mohr – Coulomb criterion is less sensitive to elasticity modulus reduction. Even if differences between numerical and experimental results are reduced, they are still important.

Vermeer's criterion indicates instead values approximating quite well the experimental bending moments.

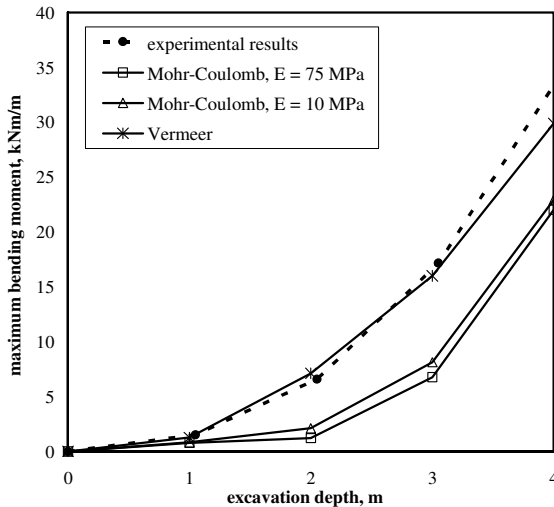


Fig. 15. Maximum bending moments in the retaining wall

Figure 16 presents bending moments in the retaining wall versus excavation depth graphs.

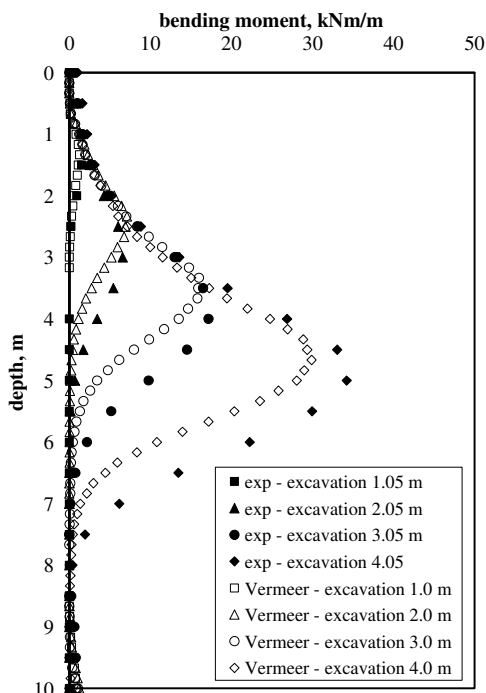


Fig. 16. Bending moments in the retaining wall

One can note a good correlation for the bending moment evolution, with a slight underestimation of the moments below the maximum moment point. This indicates a real embedment of the wall in the soil beneath the excavation level at a higher depth than that indicated by the numerical calculations. This explains also the slightly underestimated displacements which have been obtained by numerical calculations.

## 5 Conclusions

As it was demonstrated here above, using advanced constitutive laws for describing material behavior is a very important aspect in geotechnical design. The development of numerical modeling, especially FEM, allows more complex approaches.

The studied case is the one of a retaining wall, which is a common type of structure in civil engineering, used especially for deep excavations in urban areas. Soil – structure interaction is important in case of these works and an incorrect design can lead to important degradations of neighboring structures.

For these reasons using advanced models and methods is highly required. But, due to model complexity and to the large number of involved parameters, FEM calculations can lead to false results. For this reason, calibration of the parameters and validation of the numerical model are compulsory by comparing the calculation results with measurements.

Paper presents some of the essential aspects of modeling geotechnical structures using FEM, taking into consideration various constitutive laws for soils and comparing experimental and numerical results.

The advantages of using a simple constitutive law as Mohr – Coulomb criterion are obvious: easiness of the experimental determination of the law parameters, their clear influence on the soil behavior. The inconvenients are also obvious and they are related to the linear elasticity of the model. For small stresses the numerical results strongly underestimate the experimental values. Only for high stresses (excavation depths over 3 – 4 m), when the plastic response of the soil becomes important and when the structure approaches the limit state, the numerical values are closed to the experimental ones, [10].

In case of using Vermeer's criterion, things are different. The advantages of a nonlinear elastic – hardening plastic model are obvious. Differences between calculations and experiment are reduced to acceptable values. Probably, with an improvement of the numerical model, these differences could be reduced further more. The inconvenients in this case are related first of all to the determination of the model parameters. This implies complex laboratory tests which are not possible in any ordinary laboratory. As well, the influence of the parameters on the soil behavior is not clear and parameters require a calibration before being used in numerical models. This calibration is not easy, as it has been shown in the paper. Last, but not least, using Vermeer's criterion in numerical calculations led to an important increase of the calculation time, compared to Mohr – Coulomb and for excavation depths of more than 4 m we have experienced problems in calculation convergence. An improvement of the model must be

done in order to be used for higher excavation depths, close to the structure limit state.

#### References:

- [1] Heath A., A strain-based non-linear elastic model for geomaterials, *WSEAS transactions on applied and theoretical mechanics*, issue 6, volume 3, june 2008, pp. 197-206.
- [2] Ahmadi H., Kalantary F. Arabani M., A hyperbolic behaviour model for partially saturated fine soils, *Proc. of the 9<sup>th</sup> WSEAS Int. Conf. on Math. and Computational Methods in Science and Eng.*, Trinidad and Tobago, nov. 5-7, 2007, pp. 14-20.
- [3] Keshuan M., Lieyun D., Finite element analysis of tunnel-soil-building interaction using displacement controlled model, *7<sup>th</sup> WSEAS Int. Conf. on Applied Computer & Applied Computational Science (ACACOS '08)*, Hangzhou, China, april 6-8, 2008, pp. 306-311.
- [4] Azadi M.R., Nordal S., Sadein M., Nonlinear behaviour of pile-soil subjected to torsion due to environmental loads on jacket type platforms, *WSEAS Transactions on Fluid Mechanics*, issue 4, volume 3, oct. 2008, pp. 390-400.
- [5] Mestat Ph., Lois de comportement des géomatériaux et modélisation par la méthode des éléments finis, *Etudes et recherches des laboratoires des ponts et chaussées*, GT 52, 1993, 193 p.
- [6] Nova R., A model of soil behaviour in plastic and hysteretic ranges, *Int. Workshop on Constitutive Behaviour of Soils*, Grenoble, 1982, pp. 289-306.
- [7] Mestat Ph., Modélisation des sables avec la loi de Nova: détermination des paramètres et influence sur les simulations, *Bulletin des Laboratoires des Ponts et Chaussées*, 2000, 225, pp. 21-40.
- [8] Vermeer P., A five constant model unifying well established concepts, *International workshop on Constitutive Behaviour of Soils*, Grenoble, 1982, pp. 175-197.
- [9] Mestat Ph., Méthodologie de détermination des paramètres des lois de comportement des sols à partir d'essais triaxiaux conventionnels, *F.A.E.R. 1.16.21.0*, 1990, 195 p.
- [10] Popa H., Contributions to the study of soil – structure interaction for underground works. *PhD these*, 2002, Technical University of Civil Engineering of Bucharest, 311 pp.
- [11] Popa H., Thorel L., Batali L., Retaining walls in urban areas. Numerical modelling, characteristic interaction parameters”, *XIV European Conference on Soil Mechanics and Geotechnical Engineering*, 24-27 Sept. 2007, Madrid, Spain, pp. 629-634.
- [12] Popa H., Use of finite element method in retaining wall design. Model of a centrifuge test, *Proc. of XIII<sup>th</sup> European Conference on Soil Mechanics and Geotechnical Engineering*, 25-28 august 2003, Prague, pp. 545-548, vol. 3, ISBN 80-86769-02-X.
- [13] Gaudin C., Modélisation physique et numérique des écrans de soutènement autostable : application à l'étude de l'interaction écran-fondation. *Thèse de Doctorat*, Université de Nantes, 2002, 410 p.
- [14] Gaudin C., Riou Y., Popa H., Garnier J., Numerical modelling of centrifuge test on embedded wall, *Proc. 5<sup>th</sup> European Conference on Numerical Methods in Geotechnical Engineering*, September 2002, Paris, pp. 689-696.